

ANALYTICAL AND EXPERIMENTAL STUDIES OF DROPLET PLUMES WITH APPLICATION TO CO₂ OCEAN SEQUESTRATION

E. Eric Adams, Brian C. Crouse, Timothy H. Harrison, and Scott A. Socolofsky
Dept. Civil & Environ. Engrg., Massachusetts Institute of Technology,
Cambridge, MA 02139

1. Abstract

This paper describes a numerical model of a steady-state plume in linear stratification driven by a buoyant dispersed phase, such as bubbles or droplets. The model was developed specifically to simulate CO₂ sequestration plumes. It extends the hybrid double-plume model of Asaeda & Imberger (1993) by incorporating droplet dynamics (dissolution, hydrate formation, and phase changes), by introducing a self-regulating detrainment criterion, and by allowing multiple intrusions to overlap. The model is calibrated to data from the literature and is applied to study the sensitivity of a CO₂ plume to ambient stratification.

2. Introduction

Several techniques for transferring CO₂ to the deep ocean have been proposed; buoyant droplet plumes injected around 1000 m depth are the simplest and least costly (Adams & Herzog 1996). Although the oceans and atmosphere will eventually equilibrate (on the order of 1000 years), the intent of such a sequestration strategy is to minimize atmospheric CO₂ concentrations over the next few hundred years, by which point CO₂ emissions will have significantly decreased (Adams & Herzog 1996). This paper examines the design of such a CO₂ injection.

This paper presents a numerical model for a two-phase plume in stratification that extends the hybrid double-plume model of Asaeda & Imberger (1993). The model currently neglects the effects of a crossflow in order to minimize the number of dynamic processes involved. This is deemed acceptable since the no-current case probably represents a worst-case scenario in terms of dilution of the dissolved CO₂. Because the dissolution of CO₂ increases the density of the seawater, there is a feedback on the plume dynamics. After presenting the model, this paper explores the relative importance of stratification and CO₂ dissolution for controlling the resultant plume structure.

3. Model Formulation

The spatial evolution of a two-phase plume in stratification is controlled by four primary processes: buoyant forces acting upon the droplets and plume water, dissolution of the droplets, turbulent entrainment of ambient water into the plume, and buoyant detrainment, called peeling. Qualitative two-phase plume behavior depends on the values of the droplet buoyancy flux, B , droplet slip velocity, u_s , and the strength of the ambient density stratification, N . Asaeda & Imberger (1993) and Socolofsky (in prep.) have identified four classes of two-phase plumes in stratification, illustrated in Figure 1. Type 1 plumes act like plumes in unstratified surroundings, flowing to the water surface without interruption. Type 2 plumes exhibit one or more intermediate peeling events, where plume water is stripped from the rising droplets by buoyant forces. The peeled water descends until it becomes forms a neutrally buoyant intrusion flow. Type 1* is a variant of Type 2 where the droplet slip velocity is low enough that the droplets partially peel along with the plume water. A Type 3 plume occurs when the droplet slip velocity is very high, so that the droplet core does not effectively transport ambient fluid. The progression from Type 1* to Type 3 can be correlated with the dimensionless slip velocity (Socolofsky, in prep.),

$$U_N = \frac{u_s}{(BN)^{1/4}} \quad (1)$$

The vertical evolution of plume structure can be predicted with an integral model. Integral models describe the plume flow as a one-dimensional problem by assuming a profile shape independent of height for each variable describing a plume property. Although this similarity assumption is not strictly valid for a two-phase plume in stratification, models based on similarity have been successful (Asaeda & Imberger 1993, Wüest et al. 1992, Turner 1986, McDougall 1978). Here, we choose top-height profiles (variables are assumed constant over the plume width) for both the inner, rising plume of water and droplets, and for the outer, falling annular plume of water only. Asaeda & Imberger (1993) introduced this type of double plume.

We formulate the model in terms of the governing flux variables. The mass flux of bubbles, W_b , is given by their number flux, N_b , their nominal diameter, d_b , and their density, ρ_b , yielding

$$W_b(z) = \frac{1}{6} \pi d_b^3(z) N_b \rho_b(z) = Q_b(z) \rho_b(z) \quad (2)$$

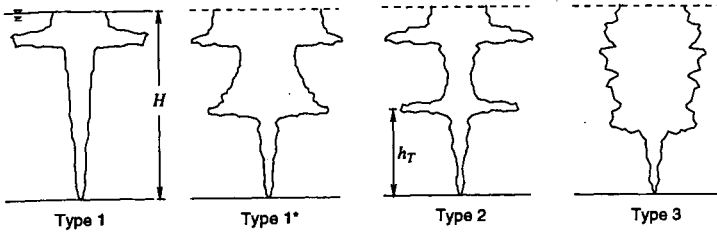


Figure 1. Schematic of characteristic two-phase plume behavior in stratification.

The size and density of bubbles are tracked in a bubble sub-model that accounts for dissolution, hydrate formation and phase changes. Denoting X as the cross-sectional fraction of the inner plume occupied by bubbles, we define the volume flux, Q , of plume water as

$$Q_i(z) = \int_0^b (1 - X(z)) u_i(z) 2\pi r dr = \pi b_i^2 u_i \quad (3)$$

where u is the average water velocity and b is the plume width. The subscript i indicates an inner-plume value. The momentum flux, M , includes the momentum of both the bubbles and the droplets

$$M_i(z) = \gamma \int_0^b (1 - X(z)) u_i^2(z) \rho_i(z) 2\pi r dr + \gamma \int_0^b X(z) (u_i(z) + u_b(z))^2 \rho_b 2\pi r dr \quad (4)$$

where u_b is the bubble slip velocity and γ is a momentum amplification term, first introduced by Milgram (1983), that accounts for the fact that the model formulation implicitly ignores turbulent momentum transport. Because $X \ll 1$ and $u_b = O(u_i)$, the second term in (4) can be ignored giving $M_i = \gamma \rho_i \pi b_i^2 u_i^2 = \gamma \rho_i Q_i u_i$.

The buoyant forces generating the plume result from changes in density. For this model, density is tracked through changes in salinity flux, S , heat flux, J , and the dissolved CO_2 flux, C . The salinity flux is defined from the local plume salinity, s , such that

$$S_i(z) = Q_i(z) s_i(z) \quad (5)$$

The heat flux of the plume is defined from the local water temperature, T , yielding

$$J_i(z) = Q_i(z) \rho_i c_p(z) T_i(z) \quad (6)$$

where c_p is the heat capacity of the fluid. Finally, the dissolved CO_2 flux is defined from the local dissolved CO_2 concentration, c ,

$$C_i(z) = Q_i(z) c_i(z) \quad (7)$$

Thus, (2) through (7) define the model state variables for the inner plume.

The state variables for the outer plume are nearly identical. The primary difference is that, because the outer plume is assumed to be annular, the volume flux of the outer plumes is defined as

$$Q_o(z) = \pi (b_o^2 - b_i^2) u_o \quad (8)$$

where the subscript, o , indicates an outer plume value. Defining z as the upward spatial coordinate and specifying that the outer plume flow downward, the velocity u_o is negative and u_i is positive. Using (8) and changing the subscripts in (2) to (7) from i to o yield the flux equations for the outer plume.

The plume develops by exchanging fluid with the ambient and by exchanging fluid between the inner and outer plumes. The entrainment hypothesis, introduced by Morton et al. (1956), states that the entrainment flux across a turbulent shear boundary is proportional to a characteristic velocity in the turbulent layer. In this model, we have defined three entrainment fluxes: E_i entrains from the ambient or from the outer plume into the inner plume, E_o entrains from the inner plume into the outer plume, and E_a entrains from the ambient into the outer plume. The entrainment relationship for counterflows is not well known. Here, we adopt the relationship used by Asaeda & Imberger (1993):

$$E_i(z) = 2\pi b_i \alpha_i (u_i - u_o) \quad (9)$$

$$E_o(z) = 2\pi b_o \alpha_o u_o \quad (10)$$

$$E_a(z) = 2\pi b_o \alpha_a u_o \quad (11)$$

where the α 's are entrainment coefficients.

The final exchange equation accounts for buoyant detrainment, which has been modeled in a variety of ways. Liro (1992) assumed that a fixed fraction of plume fluid was ejected when the net buoyancy flux across the plume approached zero. Asaeda & Imberger (1993) assumed that all of the plume fluid detrained when the net momentum approached zero. Based on experiments, peeling is better predicted when the net momentum approaches zero. For this model, a self-regulating peeling criterion is introduced. We know that peeling occurs when the drag from the bubbles can no longer support the negative buoyancy of the fluid. The simplest parameterization that behaves similarly to experiments gives the peeling flux as

$$E_p(z) = \varepsilon \left(\frac{u_b(z)}{u_i(z)} \right)^2 \left(\frac{B_i(z)}{u_i^2(z)} \right) \quad (12)$$

where ε is a non-dimensional fitting parameter of order 0.01, and B is the buoyancy flux, defined as

$$B_i(z) = gQ_i(z) \frac{\rho_a(z) - \rho_l(z)}{\rho_l} \quad (13)$$

where ρ_a is the ambient density. The relationship in (12) makes it easier for outer plumes to overlap and makes it possible to simulate the continuous peeling nature of Type 3 plumes, which were first defined by Asaeda and Imberger (1993).

With these definitions, the plume conservation equations can be readily defined. From mass conservation, we have:

$$\frac{dQ_i}{dz} = E_i + E_o + E_p \quad (14)$$

$$\frac{dQ_o}{dz} = E_i + E_o + E_p + E_a \quad (15)$$

Momentum conservation states that the momentum changes in response to the applied forces, which gives the following equations

$$\frac{dM_i}{dz} = g \left(\frac{Q_o}{(u_i + u_b)} (\rho_a - \rho_b) + \pi b_i^2 (\rho_a - \rho_l) \right) + E_i \rho_o u_o + E_o \rho_l u_i + E_p \rho_l u_i \quad (16)$$

$$\frac{dM_o}{dz} = -g\pi(b_o^2 - b_i^2)(\rho_a - \rho_o) + E_i \rho_o u_o + E_o \rho_l u_i + E_p \rho_l u_i + E_a \rho_a u_a \quad (17)$$

The conservation of salt, heat and dissolved CO₂ flux follow from the mass conservation equation, yielding for the inner plume:

$$\frac{dS_i}{dz} = E_i s_o + E_o s_i + E_p s_i \quad (18)$$

$$\frac{dJ_i}{dz} = c_p \rho_l (E_i T_o + E_o T_i + E_p T_i) + \frac{dW_b}{dz} \Delta H_{diss} \quad (19)$$

$$\frac{dC_i}{dz} = E_i c_o + E_o c_i + E_p c_i \quad (20)$$

and for the outer plume:

$$\frac{dS_o}{dz} = E_i s_o + E_o s_i + E_p s_i + E_a s_a \quad (21)$$

$$\frac{dJ_o}{dz} = c_p \rho_l (E_i T_o + E_o T_i + E_p T_i + E_a T_a) \quad (22)$$

$$\frac{dC_o}{dz} = E_i c_o + E_o c_i + E_p c_i + E_a c_a \quad (23)$$

The last term in (19) accounts for the energy released by dissolving CO₂. The densities ρ_l and ρ_o are determined by an equation of state which is a function of s , T , and c . dW_b/dz is calculated by the bubble sub-model.

The model begins with integration of the inner plume from the point of release to the point where the droplets disappear or the water surface is reached. Once the inner plume integration is complete, the outer plume segments are integrated. The integration of each outer plume section continues until the momentum flux approaches zero. Then, the next outer plume section is initialized and integrated. This cycle repeats until the solution converges to a steady result (typically 10 iterations).

4. Results

Literature data were available for an unstratified bubble plume and for a single-phase plume ($u_b=0$) in stratification. For both these cases the outer plume did not develop, so only values for α_i could be calibrated. Data for the unstratified case were from Milgram (1983) for a 50 m deep spring. The model matched the trend and magnitude of the measured plume velocities for a value of $\alpha_i =$

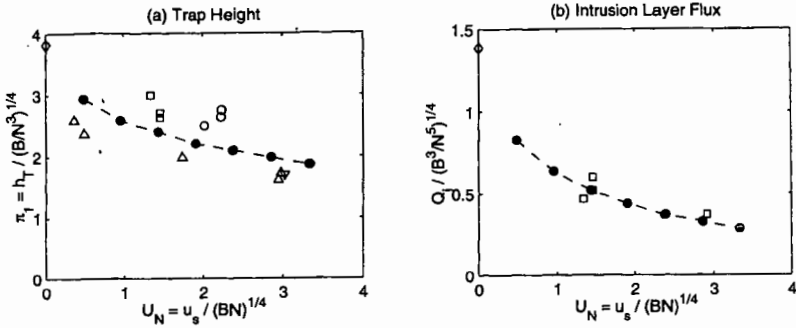


Figure 2. Model predicted (a) trap height and (b) intrusion layer volume flux versus experimental data. Up and down triangles are from Reingold (1994), open circles are from Asaeda and Imberger (1993), right-pointing triangles are from Lemckert and Imberger (1993), and squares are from experiments described in Socolofsky (in prep.). Model predictions are represented by the filled circles.

0.12. In the stratified case, the trap height relationship $h_T = 3.8(B/N^3)^{1/4}$ was tested. The model reproduced the scale-dependence of h_T on B and N for $\alpha_i = 0.11$.

Additional calibration data for two-phase plumes in stratification were available from Socolofsky (in prep.). The height of the first peeling event, h_T , and the volume flux in the resulting intrusion, Q_i , can be correlated with U_N . Calibrating to the trap-height relationship gives values of $\alpha_i = 0.07$, $\alpha_o = 0.11$, and $\alpha_s = 0.11$. Figure 2 shows the model predictions for trap height and intrusion layer flux, compared to experimental data.

The ambient density gradient, characterized by the buoyancy frequency, varies somewhat with geographic location and strongly with depth. To investigate the model sensitivity to stratification, a base-case CO_2 injection scenario was defined. Table 1 summarizes the base case along with scenarios featuring decreased and increased stratification.

Variable	Decreased Stratification	Base Case	Increased Stratification
Release Depth	800 m	800 m	800 m
Droplet Diameter	0.5 cm	0.5 cm	0.5 cm
Droplet Density	940 Kg/m ³	940 Kg/m ³	940 Kg/m ³
Flow rate	1.1 L/s	1.1 L/s	1.1 L/s
Buoyancy Frequency	0.0016 s ⁻¹	0.0032 s ⁻¹	0.0064 s ⁻¹

Table 1. Simulation scenarios for CO_2 sequestration sensitivity analysis.

Figure 3 shows the model results for the three sequestration scenarios in Table 1. Although the total plume rise heights are about the same (the bubbles completely dissolve at the same height), the intrusion levels and fluxes differ. The volume flux to the intrusion layers decreases with increasing stratification because their descent is arrested more quickly in higher stratification, which leads to less cumulative entrainment and less total dilution. The mean concentration of excess CO_2 and the resulting change in pH in the intrusions are summarized in Table 2.

Case	Intrusion excess CO_2
Decreased stratification	0.03 Kg/m ³
Base case	0.06 Kg/m ³
Increased stratification	0.13 Kg/m ³

Table 2. Intrusion excess CO_2 concentration and change in pH for the three cases simulated.

The near-field dilution of the CO_2 reported in Table 2 is controlled by the competition between the stratification and the solution density effect of the CO_2 . Over the range of buoyancy frequencies sampled, the concentration of CO_2 in the intrusion layers is nearly proportional to the buoyancy frequency.

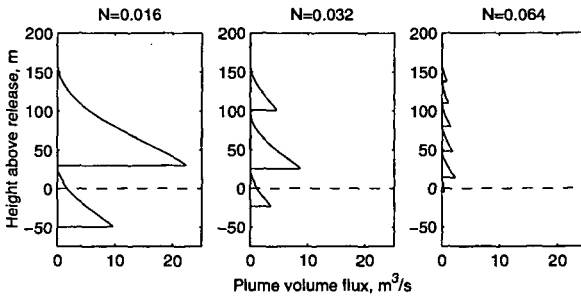


Figure 3. Sensitivity of plume structure to ambient stratification. The solid lines represent the volume flux profiles of the outer plume sections. The inner plume volume flux profiles are omitted for clarity.

5. Conclusions

A numerical model has been presented that extends our modeling abilities for a buoyant CO_2 plume in the deep ocean. The newly introduced detrainment relationship (12) provides a convenient numerical solution for downdraught flows that overlap, as is the case for CO_2 plumes. Although the entrainment relationship for the resulting counterflow is not well understood, the density feedback of the CO_2 dissolution provides a large enough driving force that the outer plume dominates the structure, and the dilution in the outer plume becomes insensitive to reasonable values for the entrainment coefficients. Thus, the near-field dilution of a CO_2 plume is controlled by the balance between the negative buoyancy of the dissolving CO_2 and the stratification, rather than by the buoyancy of the bubbles.

6. Acknowledgements

This work was supported by the MIT Sea Grant College Program, the National Energy Technology Laboratory of the U.S. Department of Energy, and the Deep Spills Task Force, comprised of the Minerals Management Service of the U.S. Department of Interior and a consortium of 13 member oil companies of the Offshore Operations Committee.

7. References

- Adams, E. E. & Herzog, H. J. (1996), Environmental impacts of ocean disposal of CO_2 , Technical Report MIT-EL 96-003, Energy Laboratory, MIT.
- Asaeda, T. & Imberger, J. (1993), 'Structure of bubble plumes in linearly stratified environments', *J. Fluid Mech.* **249**, 35-57.
- Lemckert, C. J. and Imberger, J. (1993), 'Energetic bubble plumes in arbitrary stratification', *J. Hydr. Engrg.* **119**, 680-703.
- Liro, C. R., Adams, E. E., Herzog, H. J. Modeling the Release of CO_2 in the Deep Ocean, Technical Report MIT-EL 91-002, Energy Laboratory, MIT.
- McDougall, T. J. (1978), 'Bubble plumes in stratified environments', *J. Fluid Mech.* **85**, 655-672.
- Milgram, J. H. (1983), 'Mean flow in round bubble plumes', *J. Fluid Mech.* **133**, 345-376.
- Morel, F. M. M. & Hering, J. G. (1993), *Principles and Applications of Aquatic Chemistry*, Wiley-Interscience, New York.
- Morton, B., Taylor, G. I., & Turner, J. S. (1956), 'Turbulent gravitational convection from maintained and instantaneous sources', *Proc. R. Soc. London Ser. A* **234**, 1-23.
- Reingold, L. S. (1994), An experimental comparison of bubble and sediment plumes in stratified environments, M.S. Thesis, Dept. of Civ. & Environ. Engrg., MIT, Cambridge, MA
- Socolofsky, S. A., Crouse, B. C. & Adams, E. E. (2000), 'Bubble and droplet plumes in stratification 1: Laboratory studies' in Proc. IAHR 5th Int. Symp. Strat. Flow, Vancouver, BC, July 10-13.
- Socolofsky, S. A. (in prep.), Laboratory Experiment of Multi-phase Plumes in Stratification and Crossflow, Ph.D. Thesis, Dept. Civ. & Environ. Engrg., MIT, Cambridge, MA.
- Turner, J. S. (1986), 'Turbulent entrainment: the development of the entrainment assumption, and its application to geophysical flows', *J. Fluid Mech.* **173**, 431-471.
- Wüest, A., Brooks, N. H. & Imboden, D. M. (1992), 'Bubble plume model for lake restoration', *Wat. Resour. Res.* **28**, 3235-3250.